# Sidelobe Behavior and Bandwidth Characteristics of Distributed Antenna Arrays

Kristopher Buchanan, Timi Adeyemi, Carlos Flores-Molina, Sara Wheeland, and Drew Overturf
Space and Naval Warfare Systems Center Pacific: Electromagnetics Technology Branch, San Diego CA, USA

***Abstract*—This work investigates sidelobe and bandwidth behavior of various distributed antenna arrays. Two distributions are investigated for unique capabilities in sidelobe tapering. The Bates distribution lowers the sidelobe levels while widening the main beamwidth. By contrast, the Irwin-Hall distribution lowers sidelobe levels, while maintaining mainlobe beamwidth. The three-dimensional sidelobe pattern leads to an energy redistribution. Simulated results for a Circular Lebesgue taper are provided, similar to an Irwin-Hall taper in two-dimensional angular space. A short discussion on 3dB beamwidth with relation to bandwidth properties concludes this paper.**

***Index Terms*—Antenna, arrays and distributed beamforming.**

## I. Introduction

The beamwidth of aperiodic arrays is affected by the manner in which an element population is either clustered or dispersed. The sidelobe level is determined by the abrupt change in the element distribution. For instance, if large impulses or large peaks occur in the nth derivative of the aperture excitation, the sidelobe level is on the order of -10n dB [1]. An analysis of this sidelobe behavior is provided in Table 1 where *A* is the radius of the largest dimension of the aperture *D*.

**Table 1. Sidelobe relation to $f^{(n)}_X(x)$**

| Aperture | Derivative of impulse | Peak sidelobe-dB | 3-dB Beamwidth |
|---|---|---|---|
| Inferometer | 0 | 0 | $.25\lambda / A$ |
| Complimentary Triangle \|x\| | 1 | -4.6 | $.357\lambda / A$ |
| Rectangle | 1 | -13.4 | $.443\lambda / A$ |
| Circle | 1-2 | -17.5 | $.514\lambda / A$ |
| Spherical (1-$x^2$) | 2 | -22.0 | $.578\lambda / A$ |
| Cosine | 2 | -23.5 | $.594\lambda / A$ |
| Triangle | 2 | -26.8 | $.660\lambda / A$ |
| Raised Cosine | 3 | -32.0 | $.745\lambda / A$ |

The expected value of the array factor across the interval [-1, 1] for a random variable *x* in any volumetric distribution provides the characteristic functions ($\Lambda$) in (1), which are orthogonal in all three axes and uncorrelated [2-3]. In fact, [1] has determined the main beam and first sidelobe level of the characteristic function have fairly deterministic properties. As a consequence, the same methods used in aperture theory may be applied to distributed arrays [1]. To analyze this methodology, a simplified expected pattern is used from (1) in terms of *Psi space* ($\Psi$) where $\Psi$ is taken over all angular space ($\theta$, $\phi$).[1]

$$\bar{U} = \frac{1}{N} + \left(1-\frac{1}{N}\right)\Lambda|u|^2\,\Lambda|v|^2\,\Lambda|w|^2 = \frac{1}{N} + \left(1-\frac{1}{N}\right)\Lambda\left|\vec{\Psi}\right|^2,$$
$$\Lambda = [\text{Main Lobe Factor}] = \int_{-1}^{1} f_x(x)\exp\left(jx\vec{\Psi}\right) \quad (1)$$
$$\vec{\Psi} = \cos^{-1}\left(kA\left(\hat{r}(\theta,\phi)-\hat{r}(\theta_0,\phi_0)\right)\right) = \cos^{-1}\left[u \quad v \quad w\right]$$
$$u = \hat{x}\cdot\cos\vec{\Psi}, v = \hat{y}\cdot\cos\vec{\Psi}, w = \hat{z}\cdot\cos\vec{\Psi}, 1 = \sqrt{u^2+v^2+w^2}$$

## II. Beamwidth and Sidelobe Level Discussion

### A. Bates Distribution

Any regular distribution with itself an infinite number of times will generate a Gaussian distribution.[2] This is analogous to a Bates distribution and is illustrated in Fig. 1 for uniform distributions (2). In other words, convolution of a square with itself produces a triangular distribution until its $n^{th}$ convolution converges to a bell shaped (Gaussian) distribution. On the contrary, this generates a GaussSinc taper (3) in its Fourier domain, which broadens its beamwidth characteristics while lowering sidelobe levels.

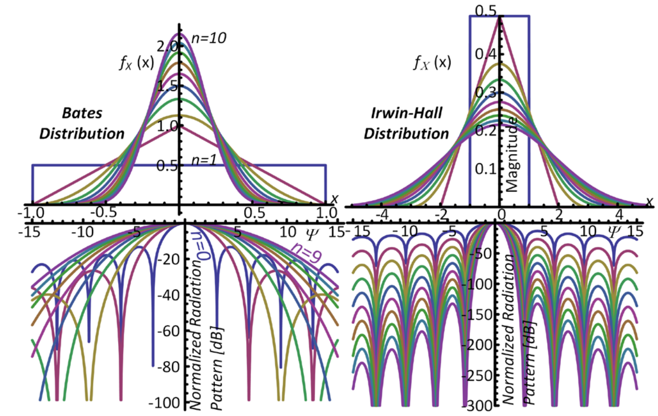


**Fig. 1. Bates distribution (top-left); Modes (bottom-left). Irwin-Hall distribution (top-right); Modes (bottom-right).**

$$f_X(x) = \frac{1}{2(n-1)!}\sum_{k=0}^{n}(-1)^k\binom{n}{k}\binom{(x-k)^{n-1}}{\operatorname{sgn}(x-k)} \neg x(0,1) \quad (2)$$

---

[1] *Psi* space is also commonly referred to *u* space [1] and [4].

[2] The exception to this rule is irregular distributions such as pulse trains that convolve into them self.

$$\Lambda(\Psi) = \mathrm{GaussSinc}_n(\Psi) = n^n\,\mathrm{Sinc}(\Psi/n)^n \quad (3)$$

### B. *Irwin-Hall Distribution*

The well-known Irwin-Hall distribution (4) is similar to the preceding Bates distribution. However, the Irwin-Hall sums the distribution from [-1, 1] as the Bates distribution finds the mean between the interval [-1, 1]. In other words, self-convolutions expand the distribution horizontally rather than vertically, as seen in Fig 1. Likewise, its Fourier modes are provided in (7) and are denoted IrwinSinc modes. These modes dampen sidelobe levels with minimal impact to mainlobe beamwidth. Instead energy is uniformly spread to the three-dimensional sidelobe pattern.

$$f_X(x) = \frac{n}{2(n-1)!}\sum_{k=0}^{n}(-1)^k\binom{n}{k}\left(\frac{(nx-k)^{n-1}}{\mathrm{sgn}(nx-k)}\right)x(0,\mathrm{n}) \quad (4)$$

$$\Lambda(\Psi) = \mathrm{IrwinSinc}_n(\Psi) = \mathrm{Sinc}(\Psi)^n \cup \Re^1 \quad (5)$$

### C. *Lebesgue Taper*

A Lebesgue space is comparable to an Irwin-Hall distribution with Fourier distributions that are analogous to an integral in a Banach space.[3] Fig. 1 illustrates the superellipse distributions, which all mathematically describe a unit circle of different Lebesgue spaces ($L^P$). In other words, different p-norms apply different length formulas which are different from the common Euclidean length $L^2$ norm.

Simulated results of the Fourier domain, $L^P$ distributions are provided in Fig. 2. These patterns illustrate pattern integrity for $n < 2$ similar to the Irwin-Hall patterns of Fig 1. However, grating lobes are induced for large $n$. This increment causes the distribution space to become discontinuous, periodic and equivalent to grating lobes encountered in large interelement spacings of periodic arrays.

### D. *Angular Space Beamwidth Comparisons*

In [4] the 3 dB beamwidth (6) and relative bandwidth (7) of a spherical random array with uniformly distributed element population are equivalent in $\Psi$ space.

$$\Psi(\tilde{A})_{av}^{3dB} = 2\arcsin(.1444\lambda/A) \approx .578\lambda/A = 16.5^{\circ}/\tilde{A} \quad (6)$$

$$\Psi(B/f)_{av}^{3dB} = 2(\Delta f/f)_0 \approx .578/\tilde{A} \quad (7)$$

where the array bandwidth $B = 2\,\Delta f$, and $\Delta f$ is the differential frequency span from its center frequency $f_0$. Likewise, the 3dB bandwidth is independent of $f$ and is characteristic of the topology such that $B=2(\Delta f)_0=.578\ c/A$.

Fig. 3 verifies these results. A spherical random array (*SRA*) maintains pattern integrity amongst scanning due to its symmetry in effective aperture whereas the circular random array (*CRA*) and linear random array (*LRA*) patterns do not. In fact the mainbeam of a CRA can be seen to adjoin at the end fire direction ($\theta_0=90°$) with its alias or back-beam, which distorts its resolution. The LRA is similar, but has a square pattern in both $\phi$ and $\theta$-cut-planes [2]. Moreover, the 3dB beamwidths of the LRA, CRA and SRA were found graphically in $\theta$, $\phi$ space in order to determine true bandwidth capabilities of the arrays. Results are provided in Table 2 for half power beamwidth and Table 3 independent of center frequency and unity aperture ($A$=1).

A final note compares periodic arrays which are nominally limited in bandwidth by electrical spacing. However, random antenna arrays are frequency independent in terms of electrical spacing. Bandwidth is merely affected by the element factor.

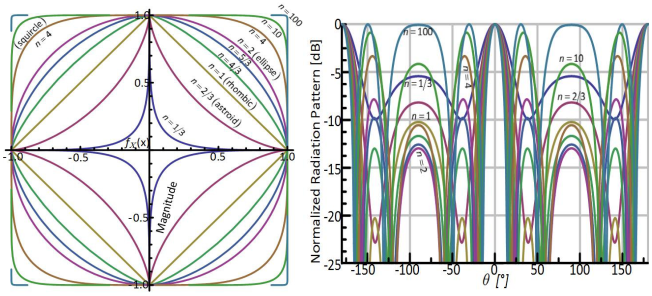


**Fig 2. Superellipse distribution functions (left); characteristic functions (right-[numerical results]).**

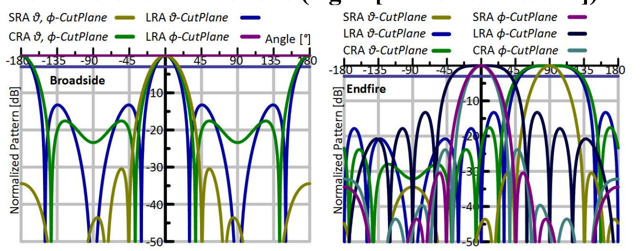


**Fig 3. LRA, CRA, and SRA scans in angular ($\theta$, $\phi$) space; Broadside ($\theta_0$=0°, $\phi_0$=0°), left and endfire ($\theta_0$=90°), right.**

**Table 2. 3dB beamwidths for a LRA, CRA and SRA**

| Broadside ($\theta_0$=0°, $\phi_0$=90°) | | Endfire ($\theta_0$=90°, $\phi_0$=90°) | |
|---|---|---|---|
| $\theta$-CutPlane | $\phi$-CutPlane | $\theta$-CutPlane | $\phi$-CutPlane |
| 38.85° λ *LRA* | 38.85° λ | 12.79° λ | Undefined |
| 41.98° λ *CRA* | 14.79° λ | 14.90° λ | 14.90 λ ° |
| 16.64° λ *SRA* | 16.64° λ | 16.64° λ | 16.64° λ |

**Table 3. Bandwidth comparison in angular ($\theta$, $\phi$) space.**

| Broadside ($\theta_0$=0°, $\phi_0$=90°) | | Endfire ($\theta_0$=90°, $\phi_0$=90°) | |
|---|---|---|---|
| $\theta$-CutPlane | $\phi$-CutPlane | $\theta$-CutPlane | $\phi$-CutPlane |
| 133.92 MHz | ∞ | 406.86 MHz | 406.86 MHz |
| 156.06 MHz | 156.06 MHz | 219.81 MHz | 154.86 MHz |
| 173.82 MHz | 173.82 MHz | 173.82 MHz | 173.82 MHz |

[3] $\boldsymbol{\Re^n}$ together with the *p-norm* is a Banach space and this Banach space is the $L^p$-space over $\boldsymbol{\Re^n}$.

## REFERENCES


[1] B. D. Steinberg, Principles of Aperture & Array System Design, New York: Wiley, 1976.

[2] K. R. Buchanan, "Theory and applications of aperiodic (random) phased arrays," Ph.D. dissertation, Dept. Elect. & Com. Eng., Texas A&M University, TX, 2014.

[3] K. Buchanan and G. Huff, "A stochastic mathematical framework for the analysis of spherically bound random arrays," *IEEE Trans. Antennas Propag.,* vol. 62., pp. 3002-3011, June 2014.

[4] T. A. Dzekov and R. S. Berkowitz, "Parameters of a spherical random antenna array," in Electron. Lett., vol. 14, no. 16, pp. 495-496, Aug. 1978.